

Friction and wear behaviors of Fe-14Mn-9Cr-5Ni-6Si and Fe-13Cr-12Co-8Mn-6Ni-6Si shape memory alloys

Amine Charfi*, Mohamed Trabelsi & Mohamed Kharrat

University of Sfax, Laboratory of Electromechanical Systems (LASEM-ENIS), Sfax (Tunisia)

Received: 23 May 2018; Accepted: 26 July 2019

Iron-based shape memory alloys are the materials that can be especially used in civil engineering structures and pipe coupling because of their good mechanical properties and their low price compared with Ni-Ti and copper-based alloys. However, their applications have been remained limited so it is very important to determine the wear behaviours of this family of materials. This paper presents friction and wears behaviours of Fe-14Mn-9Cr-5Ni-6Si and Fe-13Cr-12Co-8Mn-6Ni-6Si under both dry and lubricated conditions by means of reciprocating ball-on-flat tribometer. The aim of this study is to determine the influence of chemical composition of iron-based shape memory alloys on tribological behaviours of material and compare their behaviours with that of Fe-32Mn-6Si which is considered as a basis reference. Morphologies and microstructures of specimens have been characterized by optical microscope. The wear tests and the optical micrograph observations of studied alloys have shown that the tribological behaviors of shape memory alloys depend on the chemical composition of material which is mainly influenced by the presence of nickel, chromium and cobalt in material. The results have shown that friction coefficients of Fe-14Mn-9Cr-5Ni-6Si and Fe-13Cr-12Co-8Mn-6Ni-6Si are almost equal and less than of Fe-32Mn-6Si. Moreover, the addition of cobalt in the chemical composition of shape memory alloys reduces considerably the stick-slip phenomenon. It has been also shown that wear resistance of alloys in oily friction is higher than that in dry friction.

Keywords: Iron-based shape memory alloys, Friction behavior, Wear behavior

1 Introduction

Iron based shape memory alloys (SMAs) are very interesting to use because of their low cost, their high mechanical strength, fine workability¹ as well as their good tribological properties². Despite their distinctive properties, iron-based shape memory alloys are currently used only in a few practical applications such as tighteners or pipe couplings³ and civil engineering⁴ such as in buildings of bridges⁵. These materials can be used also as external end-fixed reinforcements to strengthen reinforced concrete structures⁶. For these applications, the wear performance of material plays an important role in ensuring its durability. The shape memory effect of iron based shape memory alloys is explained by the reverse transformation of the hexagonal (ϵ) martensite to the face centered cubic (fcc) (γ) austenite phase⁷. Iron based shape memory alloys are limited by their poor corrosion resistance⁷⁻⁹, the addition of chromium, nickel and cobalt improve this chemical property. However, the cost of these new nuances becomes less attractive for many applications^{10,11}. In Fe-Mn-Cr shape memory alloys, a

high quantity of Cr increases the stacking fault energy and suppresses the formation of martensite which allows the stability of austenite¹².

Many research works have been carried out on Ni-Ti in regards to welding and joining¹³, physical metallurgy¹⁴, finite element modeling of Ni-Ti orthodontic wires¹⁵ and fatigue study of thin films¹⁶. Others research works have been done on copper-based alloys that can replace NiTi in many applications for their reduced cost and excellent super elasticity. These materials have shown their efficiencies essentially for damping systems in seismic devices¹⁷.

For iron-based shape memory alloys, studies were interested in the factors that promotes the martensitic transformation such as thermo-mechanical training^{18,19}, effect of the pre-deformation²⁰ and characterization of wear resistance^{21,22}. Authors concluded that wear rate decreases with hardness of materials^{22,16}. For Fe-17Mn-5Si-10Cr-4Ni alloys, Chengxin et al. Observed the presence of large amounts of martensite in the worn surface of alloys in oily friction, which is on the contrary in dry friction²¹. The high wear resistance of iron-based shape memory alloys in oily friction is the result of the stress-induced martensitic

*Corresponding Author (E-mail: charfiamin33@gmail.com)

transformation². The nitriding effect of Fe–30Mn–6Si–5Cr was studied by H.C. Lin et al., this treatment exhibits a lower weight loss than non-treated material. The nitrided layer improves the cavitation erosion resistance of alloys²³. D. Bu and all shows that ageing with pre-deformation improves the wear resistance of Fe-Mn-Si-Cr-Ni-Ti-C alloy more effectively than ageing without pre-deformation, especially under heavy load condition²⁴.

In this paper, we try to evaluate the tribological behavior of Fe-14Mn-9Cr-5Ni-6Si and Fe-13Cr-12Co-8Mn-6Ni-6Si alloys under both dry and lubricated conditions using a reciprocating linear tribometer. Moreover, the evolutions of the friction coefficient, the wear rate and wear process, for each of the considered alloys, with respect to the number of sliding cycles were analyzed.

2. Experimental Procedure

2.1. Specimens preparation

Specimens of alloys that have been used in this study are water quenched at a temperature of 1373 K. After that, the specimens present a duplex structure of austenite and marten site. The chemical composition of the material is given in Table 1. The used specimens have been cut (20 mm x 10 mm x 3 mm) by the means of electro-erosion machining along the bar direction. After this treatment, specimens were polished mechanically, have been maintained at 873 K during one hour and water cooled to room temperature. After this treatment, alloys showed a fully austenitic structure at room temperature^{25,26}.

2.2. Optical micrograph of alloys

LEICA DMILM optical microscope (OM) was used to observe the microstructure features of specimens before and after the wear test. Figure 1 shows the metallographic observations of A1 and A2. From Fig. 1, it can be seen that the microstructure of A1 presents a fully austenitic structure. The grain boundaries are well defined. For A2, we notice a duplex structure of austenite and ϵ -marten site phases. The grain size for A1 and A2 are indicated in Table 2. From Table 2, we notice that the average value of diameter for A1 is 40 μm and A2 is 15 μm . The grain size of A2 alloy is smaller than that of A1 alloy. This result shows that the addition of cobalt reduces the grain size of material.

2.3. Wear test

Tribological tests were performed using a reciprocating ball-on-flat tribometer (Fig. 2). The

dimensions of the used specimens are 20x10 x 3 mm³. The contact load between the steel ball and the specimen was assured under a constant normal load. The counter-face was high chromium steel ball (100Cr6) with a surface roughness of 0.06 μm and a radius of 19 mm. The steel ball was retained stationary and tangential cyclic motion was applied to the sample using crank system driven by an electric motor and electronic speed regulator. The tangential displacement amplitude and frequency were fixed before the start of the test. A load cell that is located between the specimen holder and the slider of the crank system were used to measure the tangential force between ball and specimen. The output of the load cell was stored by using a data acquisition system. Before each test, the sample and the ball surfaces were cleaned with ethanol. Each test was repeated three times to ensure the reproducibility of results. The surface morphology of the wear track was examined by using the optical microscope. The friction and wear test conditions are indicated in Table 3.

After wear test, the cross-section S (mm²) of the wear groove on the alloys sample was calculated from the established surface profile using SJ-210 Hand-held Roughness Tester. The volume loss V (mm³) of sample due to the wear was calculated as:

$$V = S \times d \quad \dots (1)$$

Where $d = 15\text{mm}$ is the length of the sliding stroke and S is the cross section (mm²).

Table 1 — Chemical composition of studied alloys (in wt %).

	Fe	Mn	Si	Cr	Ni	Co
A1	Bal.	18	5	8	5	-
A2	Bal.	8	6	13	6	12

Table 2 — Grain size values for studied alloys²⁷.

Alloy	grain size (μm)
A1	40 \pm 10
A2	15 \pm 5

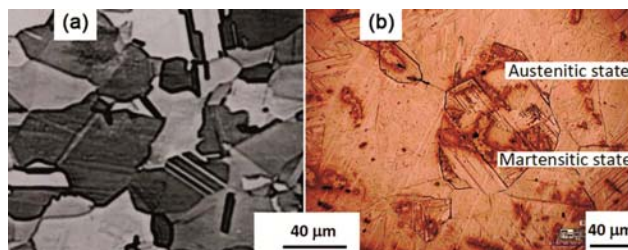


Fig. 1 — Optical micrograph of A1 and A2.

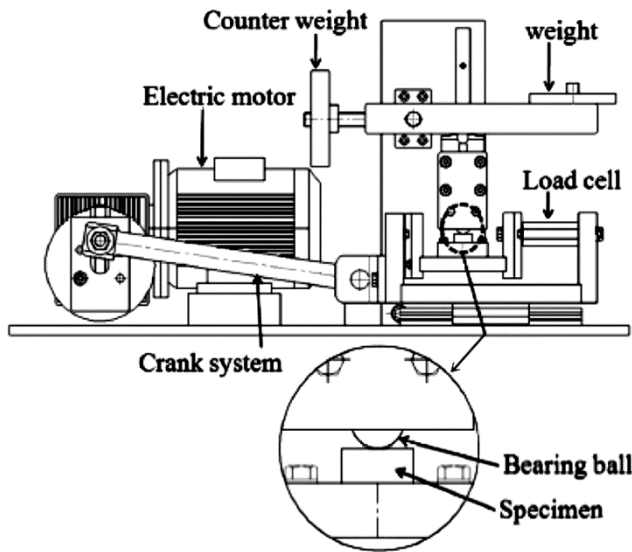


Fig. 2 — Reciprocating ball-on-flat tribometer.

Table 3 — Parameters of tribological tests.

Parameters	Values
Normal load (N)	81.3
Displacement amplitude (mm)	7.5
Frequency (Hz)	1
Temperature (°C)	20 - 25
Humidity (%)	50 - 60

The specific wear rate K (mm^3/Nm) was calculated using equation 2:

$$K = V / (F_n \times L) \quad \dots (2)$$

Where F_n the normal load (N), L the sliding distance (m) and V the volume loss (mm^3).

3. Results and Discussion

3.1 Hardness tests

The results of the hardness tests measured on A1, A2 and Fe-32Mn-6Si samples are shown in the Table 4. We notice that the hardness value for Fe-32Mn-6Si alloy is equal to 180HV, equal to 220HV for A1 and 240HV for A2. We can conclude that the presence of chromium and nickel increases the hardness of alloy as mentioned elsewhere²⁸. Moreover, the A2 alloy's hardness is slightly higher than A1 alloy. This result is explained by the presence of cobalt in material.

3.2. Friction and wear properties

3.2.1. Friction behaviours

Figure 3 shows the typical evolution of the friction coefficients of A1 and A2 against cycles number

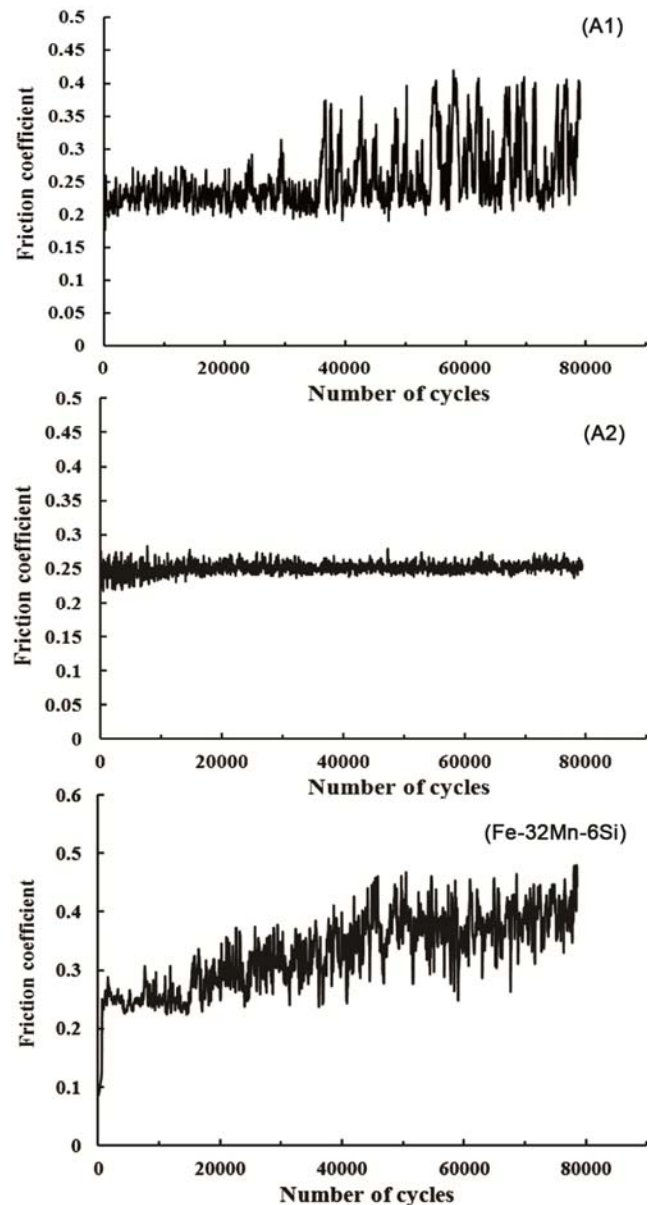


Fig. 3 — Variation of the friction coefficient against the cycle number for A1, A2 and Fe-32Mn-6Si under a load of 81.3 N.

Table 4 — Hardness values of Fe-32Mn-6Si, A1 and A2²⁷.

	Fe-32Mn-6Si	A1	A2
Hardness ($\pm 10\text{HV}$)	180	220	240

under 81.3N as normal load. As shown in the figure, for A1, in the first stage it can be seen that the friction coefficient is almost constant and equal to 0.22 with a stable friction behavior until reaching about 35000 cycles. After this cycle number value, we notice a remarkable increase of stick-slip phenomenon represented by fluctuations. This can be attributed to the fact that during the sliding test the roughness of

both surfaces in contact became important, the asperities were plastically deformed under both the normal load and the shear stress or to the chemical adhesion between the Cr-Ni alloy surface and the 100Cr6 steel ball. Consequently, micro joints take place between sample and counter-face.

For A2, we note that friction coefficient is stable throughout the test and equal to 0.25. Furthermore, the stick-slip phenomenon is not significant. For Fe-32Mn-6Si alloy, the friction coefficient gradually increases until 40000 cycles, after which the friction coefficient is stabilized at a value around 0.4 until the end of the test²⁹. The comparison of friction behaviors of A1 and A2 alloys with Fe-32Mn-6Si allows conclude that the addition elements present in these materials have improved the friction behaviors of alloys. In addition, the presence of cobalt leads to steady friction behavior with removing of the stick slip phenomenon. In fact, the friction coefficient of shape memory alloy depends on different factors related to the composition of material^{10,30}.

3.2.2 Wear behaviors

Figure 4 shows the typical profiles of the wear groove for A1 and A2 using the hand-held roughness tester after 80000 cycles of dry sliding. From the typical profiles of the wear grooves, for A1 and A2, the cross section S (mm^2) of the wear grooves were calculated. The volume loss was then plotted against the number of cycles as represented in Fig.5 for each of the considered alloys. The specific wear rate K was also plotted against the number of cycles in Fig.6.

Figure 5 shows the variation of the volume loss for A1 and A2 against cycle's number. It can be seen, for the two alloys that the volume loss increases linearly with the cycle's number until the end of the test, so the wear behavior of A1 and A2 can be described by Arc hard theory. Figure 6 shows the evolution of the wear rate of A1 and A2 as a function of cycles number. The figure shows an increase of the wear rate of materials with time. In fact, the wear resistance of the shape memory alloys degrades almost linearly when the number of cycles increases. Moreover, after 80000 cycles of sliding, the wear rate of A1 alloy, which is almost equal to 6×10^{-5} and 8×10^{-5} for A2, are less than that of Fe-32Mn-6Si alloy²⁹ which is equal to 6.3×10^{-3} . This can be explained by the presence of chrome, nickel and cobalt that improve the hardness of the material and influence both the friction and wear behaviors.

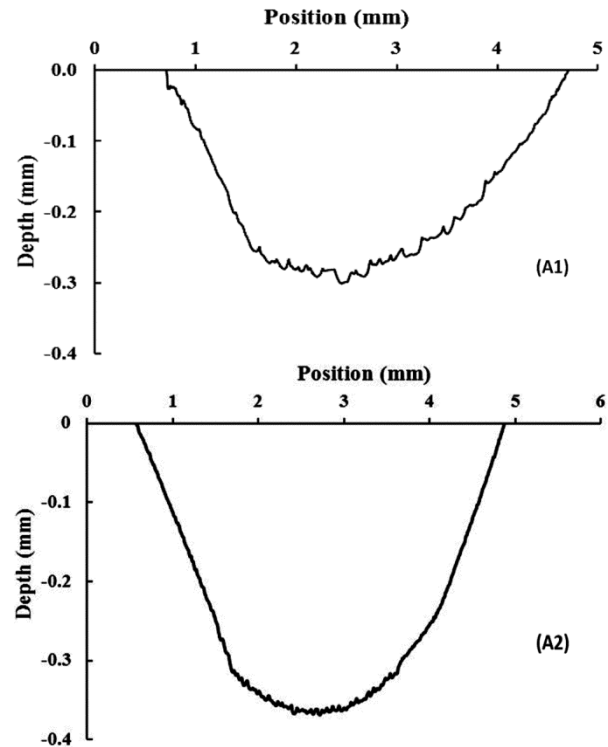


Fig. 4 — Typical profiles of the wear groove for A1 and A2.

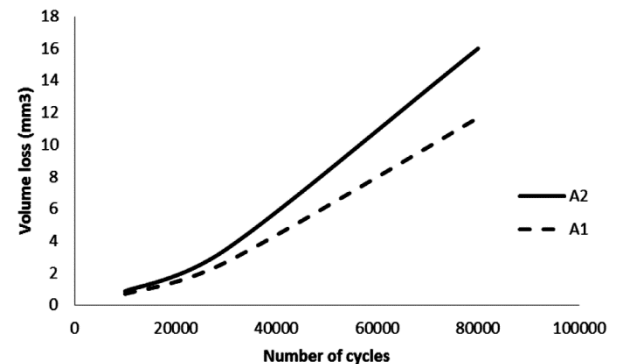


Fig. 5 — Evolution of the volume loss against the cycle number for A1 and A2.

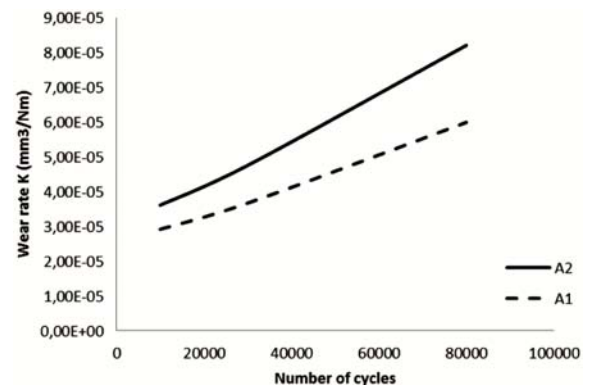


Fig. 6 — Evolution of the wear rate against the number of cycles.

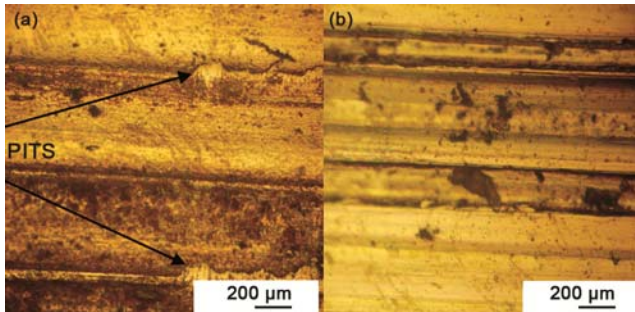


Fig. 7 — Optical micrographs of the worn surface for A1 and A2 after 80000 cycles.

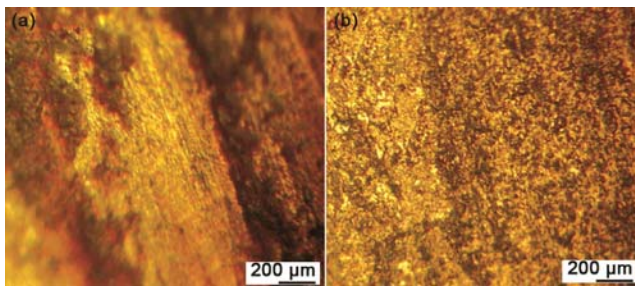


Fig. 8 — Optical micrographs of the counterface for A1 and A2 after 80000 cycles.

Figure 7 shows the optical micrographs of the worn surfaces for A1 and A2 specimens after 80,000 cycles. We observe the presence of wear grooves on the both surfaces of A1 and A2 specimens. The abrasion marks were parallel to the sliding direction. For A2 specimen, the worn surface observed after 80,000 cycles was slightly grooved and none pits were observed, this approves the result obtained in Fig. 3 indicating that the friction behavior of A2 alloy is steady along the friction test. For A1 sample, we note the presence of pits on the worn surface as it is shown in Fig. 7. On the other hand, a transfer film can be seen on the surface of the ball as it is shown in Fig. 8. This result approves the adhesion between the surface of the A1 alloy and 100Cr6 steel ball.

3.3. Effect of lubrication on wear behaviors

Figure 9 presents the variation of friction coefficient against cycle's number for A1 and A2 under lubrication. The lubricant used is the paraffin oil. It can be seen that the friction coefficients of A1 and A2 are steady around a value of 0.15. Thus the lubrication improves the friction behaviors of the two alloys. Also, the friction behaviors of A1 and A2 have become similar under lubrication. This was due to the adsorbed oil film on the surface of the sample. Figure 10 shows a smooth worn surface for A1 and a slightly grooved surface for A2. We can conclude that the

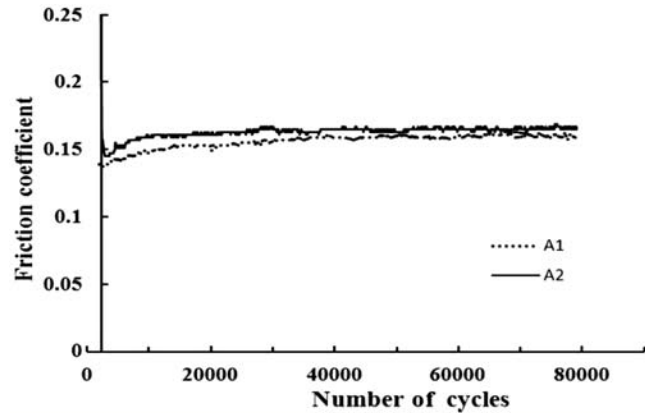


Fig. 9 — Variation of friction coefficient against the cycle number under lubrication.

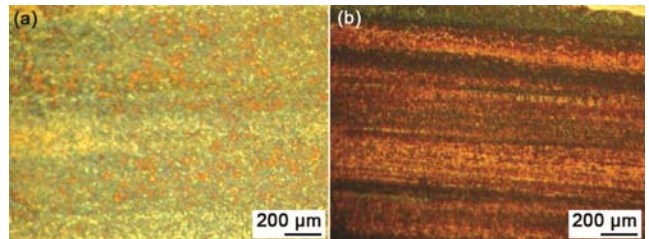


Fig. 10 — Optical micrographs of worn surface for lubrication test after 80000 cycles.

adhesion mechanism for A1 was limited by lubrication. However, for A2, the abrasion mechanism is always the same.

4 Conclusions

The tribological behavior of Fe-14Mn-9Cr-5Ni-6Si and Fe-13Cr-12Co-8Mn-6Ni-6Si shape memory alloys is determined. These nuances of materials are characterised by a good corrosion resistance and good mechanical properties. Therefore, wear and friction behaviors of Fe-14Mn-9Cr-5Ni-6Si and Fe-13Cr-12Co-8Mn-6Ni-6Si were investigated using a reciprocating ball-on-flat tribometer. The effect of lubricant on tribological behaviour was also studied. The results show that tribological behavior of studied materials is better than that of Fe-32Mn-6Si, which are considered as reference in iron-based shape memory alloys. These results are due to the effect of the addition elements such as chromium, nickel and cobalt. In dry conditions, for A1 and A2, the variation of the volume loss increases linearly with the cycle number. Thus, the wear resistance of shape memory alloys degrades almost linearly when the number of cycles increases. Results show also that wear behavior of Fe-13Cr-12Co-8Mn-6Ni-6Si is the best due to the presence of cobalt and its high value of hardness. For

Fe-14Mn-9Cr-5Ni-6Si, optical micrographs of the worn surfaces show the presence of grooves and pits. For A2, there are only slight grooves. The lubrication decreases friction coefficients of alloys and improves the friction behavior of Fe-14Mn-9Cr-5Ni-6Si and Fe-13Cr-12Co-8Mn-6Ni-6Si alloys.

References

- 1 Wan J & Chen S, *Curr Opin Solid State Mater Sci*, 9 (2005) 303.
- 2 Lin C X, Wang G X, Wu Y D, Wang J G & Zhang J J, *Mater Sci Eng A*, 420 (2006) 438.
- 3 Li J C, X X & Jiang Q, *ISIJ Int*, 40 (2000) 1124.
- 4 Cladera A, Weber B, Leinenbach C, Czaderski C, Shahverdi M & Motavalli M, *Constr Build Mater*, 63 (2014) 281.
- 5 Ghafoori E, Neuenschwander M, Shahverdi M, Czaderski Ch & Fontana M, *Constr Build Mater*, 211 (2019) 437.
- 6 Shahverdi M, Michels J, Czaderski Ch & Motavalli M, *Constr Build Mater*, 173 (2018) 586.
- 7 Lin H C, Lin K M, Lin C S & Ouyang T M, *Corros Sci*, 44 (2002) 2013.
- 8 Charfi A, Gamaoun F, Bouraoui T, Bradai C & Normand B, *Adv Mater Res*, 476 (2012) 2162.
- 9 Charfi A, Bouraoui T, Feki M, Bradai C & Normand B, *C R Chimie*, 12 (2009) 270.
- 10 Soderberg O, Liu X W, Yakovenko P G, Ullakko K & Lindroos V K, *Mater Sci Eng A*, 273 (1999) 543.
- 11 Wang Z & Zhu J, *Mater Sci Eng A*, 358 (2003) 273.
- 12 Mertinger V, Benke M & Nagy E, *Mater Today Proceed 2S* (2015) S673.
- 13 Oliveira J P, Miranda R M, Braz Fernandes F M, *Prog Mater Sci*, 88 (2017) 412.
- 14 Otsuka K & Ren X, *Prog Mater Sci*, 50 (2005) 511.
- 15 Ben Naceur I, Charfi A, Bouraoui T & Elleuchkh, *J Biomech*, 47 (2015) 3630.
- 16 Hou H, Tang Y, Hamilton R F & Horn M W, *J Vac Sci Technol A*, 35 (2017) 041602.
- 17 Oliveira J P, Zeng Z, Omori T, Zhou N, Miranda R M & Braz Fernandes F M, *Mater Des*, 98 (2016) 280.
- 18 Chung C Y, Chen S & T Y Hsu, *Mater Charact*, 37 (1996) 227.
- 19 Xia R D, Liu G W & Liu T, *Mater Lett*, 32 (1997) 131.
- 20 Baruj A, Kikuchi T, Kajiwaru S & Shinya N, *Mater Trans JIM*, 43 (2002) 585.
- 21 Chengxin L, Guixin W, Yandong W, Jingang W & Jianjun Z, *Mater Sci Eng A*, 438 (2006) 804.
- 22 Gopi V, Sellamuthu R & Arul S, *Procedia Eng*, 97 (2014) 1355.
- 23 Lin H C, Lin K M, Chen Y S & Yang C H, *Surf Coat Technol*, 194 (2005) 74.
- 24 Bu D, Peng H, Wen Y & Li N, *Mater Des*, 32 (2011) 2969.
- 25 Zhu X & Zhang Y, *J Mater Sci Lett*, 16 (1997) 1516.
- 26 Bouraoui T, Tamarat K & Dubois B, *J Phys III*, 6 (1996) 831.
- 27 Bouraoui T, *Martensitic transformations followed by electrical resistance and plasticity transformation measurement. Design and production of devices. Applications for Fe-Mn-Si shape memory steels*, Paris, 1996 (Ph. D. thesis).
- 28 Lemma J D, Warmuth A R, Pearson S R & Shipway P H, *Tribology Int*, 81 (2015) 258.
- 29 Charfi A, Trabelsi M & Kharrat M, *J Mater Educ*, 41 (2019) 59.
- 30 Saravanan R & Sellamuthu R, *Procedia Eng*, 97 (2014) 1348.